Effect of Rubber under FWD Loading Plate by Numerical Simulation

T. Nishiyama
NIPPO Corporation, Research Institute, Tokyo, Japan

S. Omoto
NIPPO Corporation, Research Institute, Tokyo, Japan

K. Matsui
Tokyo Denki University, Saitama, Japan

ABSTRACT: The detail investigation regarding FWD load transit to pavement surface is uncertain whether the applied load is equally distributed to the pavement surface or not, hence the effect of rubber on surface deflection is uncertain either. In this study, to investigate the effect of rubber beneath loading plate, numerical analyses for the following three loading cases were conducted: 1) Uniformly distributed load applied on the pavement surface, 2) Load applied through rigid plate to the pavement surface, 3) Load applied through rigid plate with rubber beneath to the pavement surface. Dynamic response analysis was conducted by FEM and deflections beneath the loading plate were calculated to investigate how the rubber affected the results of analysis. It was confirmed that the analyzed deflections at the pavement surface were different among those of three loading cases. Furthermore, dynamic backcalculation was carried out using in-situ FWD data to estimate Young's moduli and damping coefficients of pavement layers.

KEY WORDS: FWD, Dynamic backcalculation, Rubber, Rigid plate, Loading plate.

1 INTRODUCTION

Traffic environment has been changed and the trend of infrastructure requirement has shifted to environmentally friendly aspects. A lot of pavement technologies that have various kinds of unique function were developed by engineer's historically accumulated knowledge, technology, and experiment. For these unique pavements, the method of evaluation for

pavement diagnostic tool varies. A non-destructive testing device has been widely used to evaluate pavement integrity and condition. FWD is the most representative non-destructive tool and able to diagnose pavement conditions with minimum efforts.

Taking advantage that FWD data was time series deflection data at several sensor positions, the dynamic Backcalculation software (DBALM) was developed, which could simultaneously estimate Young's moduli and damping coefficients of each pavement layer (Matsui 1997). Recently, its function was expanded by adding one more parameter so that densities of each layer could also estimate (Nishiyama 2008).

As for FWD load transit, no verification has done whether the applied load is equally distributed to the pavement surface, thus the effect of rubber on surface deflection is uncertain either. In this study, to investigate the effect of rubber beneath loading plate, numerical analyses for the following three loading cases were conducted: 1) Uniformly distributed load applied on the pavement surface, 2) Load applied through rigid plate to the pavement surface, 3) Load applied through rigid plate with rubber beneath to the pavement surface. Dynamic response analysis was conducted by FEM using axisymmetric eight node quadratic elements. Deflections beneath the loading plate were calculated to investigate how the rubber affected the results of analysis. Furthermore, dynamic backcalculation was carried out using in-situ FWD data to estimate Young's moduli and damping coefficients of pavement layers.

2 DISPLACEMENT IN SOIL AND DYNAMIC RESPONSE ANALYSIS

2.1 Boussinesq Theory of Displacement in Semi-infinite Soil

According to Boussinesq theory, the shape of displacement distribution in semi-infinite structure depends on loading plate types that are either uniformly distributed load type or rigid plate type. Equation 1 indicates the theoretical vertical surface displacement at the center of uniformly distributed load in the semi-infinite soil. Equation 2 is of the rigid plate load as well as Equation 1.

$$\delta = -\frac{2P_{av}a\left(1-\nu^2\right)}{E}\int_0^\infty \frac{1}{\xi}J_1(\xi a)J_0(\xi r)d\xi \tag{1}$$

$$\delta = -\frac{\pi\left(1-\nu^2\right)P_{av}a}{2E} \tag{2}$$

where, δ : vertical surface displacement of circle, r: radial distance from center, a: radius of circle, P_{av}: average applied pressure, E: elastic modulus, ν : Poisson's ratio, J_1: 1st order of Vessel function, J_0: 0th order of Vessel function.

Dividing Equation 1 by Equation 2 and if $r = 0$

$$\frac{\rho_z^r}{\rho_z^u} = \frac{\pi}{4} \tag{3}$$

This indicates that the theoretical vertical displacement of the center of rigid plate loading at the surface is $\frac{\pi}{4}$ times smaller than that of uniformly distributed load.

2.2 Dynamic Response Analysis

The standard pavement structural system consists of surface, base, sub-base and subgrade layers. The surface base and sub-base layers are finite in thickness and infinite in extent in the horizontal direction. Subgrade layer is semi-infinite in vertical direction. Each layer material property is assumed linearly elastic. FWD test measures the pavement surface deflection wave propagation which is caused by the impact loading of weight drop. The pavement response can be analyzed by FEM. The material properties in each pavement layer are assumed uniform. Individual element has mass, damping and stiffness matrix. Using these matrices, each layer mass, damping and stiffness matrices are assembled. The j^{th} layer equation of motion is

$$\rho_j \overline{\mathbf{M}}_j \ddot{\mathbf{z}}(t) + c_j \overline{\mathbf{Q}}_j \dot{\mathbf{z}}(t) + E_j \overline{\mathbf{K}}_j \mathbf{z}(t) = \mathbf{f}_j(t) \tag{4}$$

where $\overline{\mathbf{M}}_j$, $\overline{\mathbf{Q}}_j$, $\overline{\mathbf{K}}_j$, $(j = 1, \cdots, M)$ (M is number of layer) are j^{th} layer unit mass, unit damping and unit stiffness matrices whose ρ_j, c_j, E_j are 1 respectively. Hence $\rho_j \overline{\mathbf{M}}_j$, $c_j \overline{\mathbf{Q}}_j$, $E_j \overline{\mathbf{K}}_j$ are j^{th} layer mass, damping, and stiffness matrices respectively.

Since Equation 4 is the motion of equation for each layer, it is necessary to assemble each layer equation into the global motion of equation which unifies all layers into the unique system.

$$\mathbf{M}\ddot{\mathbf{z}}(t) + \mathbf{C}\dot{\mathbf{z}}(t) + \mathbf{K}\mathbf{z}(t) = \mathbf{f}g(t) \tag{5}$$

where $\mathbf{M} = [\rho_j \overline{\mathbf{M}}_j]$, $\mathbf{C} = [c_j \overline{\mathbf{Q}}_j]$, $\mathbf{K} = \lfloor E_j \mathbf{K}_j \rfloor$ are the global mass, damping, and stiffness matrix respectively. $\mathbf{f}$ is nodal load distribution vector and $g(t)$ is a scalar representation of load as function of time.

3 METHOD OF BACKCALCULATION

The objective function of back-calculation is defined as the sum of square difference between the measured deflection $u_i (i = 1, \cdots, N)$ and calculated deflection z_i.

$$J = \frac{1}{2}\sum_{p=p0}^{p1}\sum_{i=1}^{N}\left\{u_i(t_p) - z_i(\mathbf{X}, t_p)\right\}^2 \tag{6}$$

where X_j is non-dimensional parameter of each layer ρ_j, c_j, E_j.

$$X_j = \frac{\rho_j}{\rho_j^{(0)}}, \quad \text{or,} \quad \frac{c_j}{c_j^{(0)}}, \quad \text{or,} \quad \frac{E_j}{E_j^{(0)}} \tag{7}$$

$\rho_j^{(0)}$, $c_j^{(0)}$, $E_j^{(0)}$ are reference values provided beforehand. X_j is unknown parameter. N is the total number of sensors. $p0$, $p1$ are discrete number of starting point and ending point of attempt time-domain respectively. The number of layers is M and the number of unknown parameters is $3M$. By finding the X_j that minimizes Equation 6, the difference between measured and calculated deflection at the discrete point in the time-domain becomes minimum. The necessary condition of minimizing is $\partial J / \partial(dX_k) = 0$.

$$\begin{aligned}&\sum_{j=1}^{3M}\sum_{p=p0}^{p1}\left\{\sum_{i=1}^{N}\frac{\partial z_i}{\partial X_k}\frac{\partial z_i}{\partial X_j}\right\}dX_j \\ &= \sum_{p=p0}^{p1}\sum_{i=1}^{N}\left\{u_i(t_p) - z_i(\mathbf{X}, t_p)\right\}\left(\frac{\partial z_i}{\partial X_k}\right)\end{aligned} \tag{8}$$

Equation 8 is the linear simultaneous equations with respect to dX_j, $(j = 1, \cdots, 3M)$. When the rate of change $\left|dX_j / X_j\right|$ for dX_j is small enough, back-calculation is completed. Otherwise, by substituting $X_j + dX_j$ into X_j, the iterative calculation continues until it converges.

4 NUMERICAL SIMULATIONS

Dynamic response analysis to calculate the deflections beneath the FWD loading plate were conducted using two types of pavement models shown in Figure 1. The first pavement model attempted composed of a subgrade, which was assumed to be a semi-infinite medium. Another pavement model composed 3 layer horizontally parallel layers of isotropic and homogeneous materials that was designed for light traffic volume road (Top layer: asphalt concrete, 2nd layer: cement stabilized base, and 3rd layer: subgrade). Material properties used for the dynamic response analysis are shown in Figure 1.

The three types of FWD loading plate were employed to analyze the response for each pavement model; 1) “uniformly distributed load type”, where there was no loading plate and the uniformly distributed load was directly applied on the pavement surface, 2) “rubber type”, where the rigid plate and rubber are combined as loading plate, and 3) “rigid plate type”, where there was the rigid plate only as loading plate. The attempted pavement model and loading plate types are tabulated in Table 2.

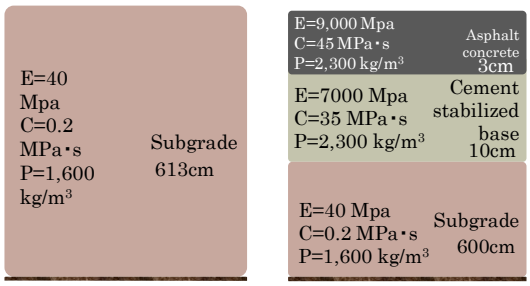

Figure 1: Semi-infinite model (left) and three layer pavement model (right)

Table 2: Pavement model and types of loading plate

Pavement model	Loading plate type	Description
Semi-infinite model	Uniformly distributed load type	No loading plate. Directly applied load on surface
	Rubber type	3cm thick rigid plate + 0.5mm thick rubber
	Rigid plate type	3.5cm thick rigid plate
3 layer pavement model	Uniformly distributed load type	No loading plate. Directly applied load on surface
	Rubber type	3cm thick rigid plate + 0.5mm thick rubber
	Rigid plate type	3.5cm thick rigid plate

The radius of loading plate was set 15 cm and thickness of rubber was set 0.5 cm as standard thickness. The thicknesses of rigid plate varied depended on types of loading plate. It was set 3 cm for rubber type and 3.5 cm for rigid plate type that was assumed to be the uniform rigid plate including rubber thickness 0.5 cm. The typical value of rubber elastic modulus was selected. The force applied for numerical simulation was artificially generated as Sine wave function with maximum value of 49 kN and regarded as FWD loading. Under these conditions, the dynamic response analysis for each pavement models and loading plate types were carried out, where the time range was from 0 to 0.04 with 0.002 sec intervals.

The method of dynamic response analysis employed was axisymmetric finite element method (FEM) using 8 nodes isoparametric elements, where each layer was discretized respectively. The entire pavement structure was discretized as shown in Figure 2 (left). The numbers of meshed elements in vertical direction of top layer, base, and subgrade were 3, 3, and 6 respectively. As shown in Figure 2 (right), the uniformly distributed load, regarding as FWD load, was directly applied on the two top elements of surface layer at the loading location. Similarly, in case of rubber type shown in Figure 3(left), the FWD load was applied directly on two rigid plate elements, located at the most top of structure, and two elements representing rubber were inserted between rigid plate and surface layer's elements. In the same way as shown in Figure 3 (right), 2 by 2 elements representing rigid plate were constructed on the surface layer elements, and FWD load was applied on the top of two rigid plate elements.

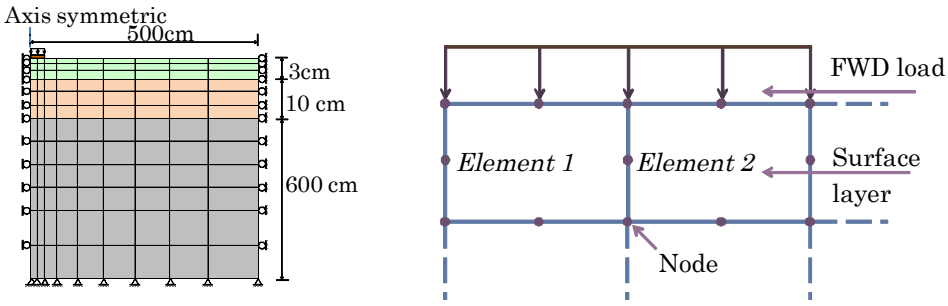

Figure 2: FEM discretized entire pavement model and near loading plate (Left: entire mesh, Right: uniformly distributed load type).

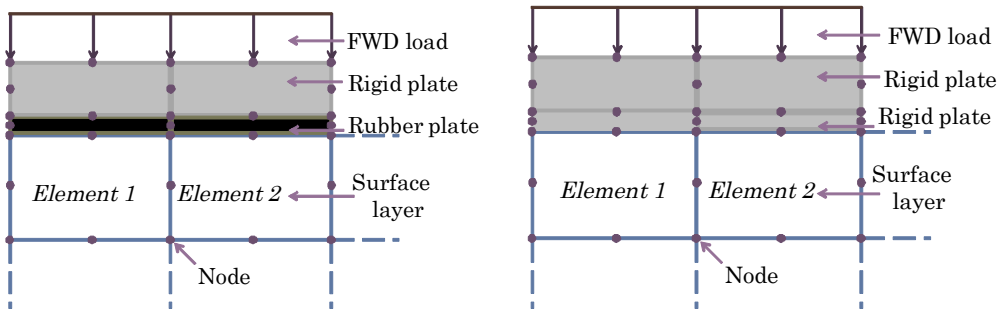

Figure 3: FEM discretized model at loading plate (Left: rubber type, Right: rigid type).

FWD device develops forces by dropping the weight of mass from a certain height. These impact forces are transmitted onto the surface of the pavement structure through the loading plate causing the pavement structure to deflect. The locations of FWD sensors which measure pavement surface deflection can be set on the surface at any desired points, however in general, the suitable sensor locations are 0, 20, 30, 45, 60 75, 90, 120, and 150 cm away from the center of loading plate. Deflections at each sensor are expressed as D0, D20, D30, D45, D60, D75, D90, D120, and D150 respectively.

The dynamic response analysis software used in this paper can calculate the deflections at any points in time domain. Especially, D0 which is the surface deflection at the center of loading plate is the most important data for stable and accurate response analysis. Hence, to evaluate the dynamic response analysis, the D0 deflection should be focused on.

For each pavement model and loading plate type as stated earlier in Table 2, the D0 deflections in time series calculated by the dynamic response analysis are plotted in Figure 4. Figure 4 (left) shows the results obtained from the semi-infinite pavement model with each loading plate types (i.e., uniformly distributed load, rubber, and rigid plate type), and Figure 4 (right) indicates of those obtained from 3 layer pavement model.

As for the results of semi-infinite model, the uniform distributed load type showed the largest deflection. Then, the rubber type had second largest deflection and rigid plate type indicated the smallest deflection. In general, the different type of loading plate induced various amount of deflections. These results showed this tendency.

Table 3 indicates the comparison results between theoretical value of Boussinesq and FEM results with respect to the ratio of D0 value obtained from uniformly distributed load to the one from rigid plate type. As derived above in Equation 3, the theoretical ratio is 0.785. On the other hand, the ratio from FEM results is 0.793. These two close values indicate that the dynamic response analysis using FEM accurately works. The D0 values between theoretical and FEM are not the same because FEM theoretically requires the finite region. Hence, the FEM meshed pavement model cannot exactly express the semi-infinite region.

Figure 5 indicates the surface deflections beneath the loading plate, where these are the maximum values (i.e., peak values) in the time domain of t = 0.0026 sec. The vertical axis is deflection and horizontal axis is the node locations between elements of loading plate and surface layer. The most left and right locations indicate the center and edge of the loading plate respectively.

As for uniformly distributed load and rubber type with respect to semi-infinite model, there exists the difference on deflection values between the center and edge of loading plate, which the deflections of edge are smaller. On the contrary, rigid plate type indicates its deflection distribution be uniform.

Result of 3 layer pavement model also shows the similar tendency to semi-finite model. The rigid plate shows slightly uneven deflection distribution. This might be caused due to the fact that the pavement model is multi-layer system and its top layer is stiff.

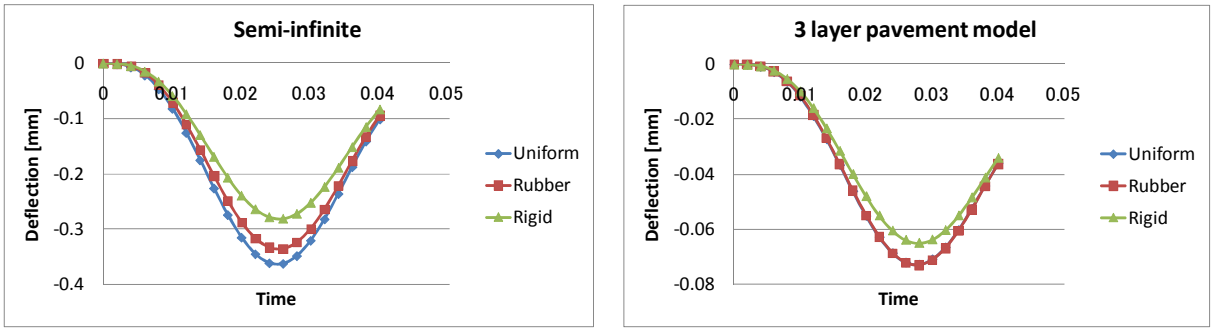

Figure 4: Deflection at sensor location of actual and calculated FWD data (Left: Semi-infinite model, Right: 3 layer pavement model).

Table 3: Deflection at D0 on both FEM and Boussinesq theoretical result of each loading type

	Uniformly distributed load	Rigid plate type	Ratio
FEM	0.363 cm	0.288 cm	0.793
Boussinesq	0.434 cm	0.341 cm	0.785

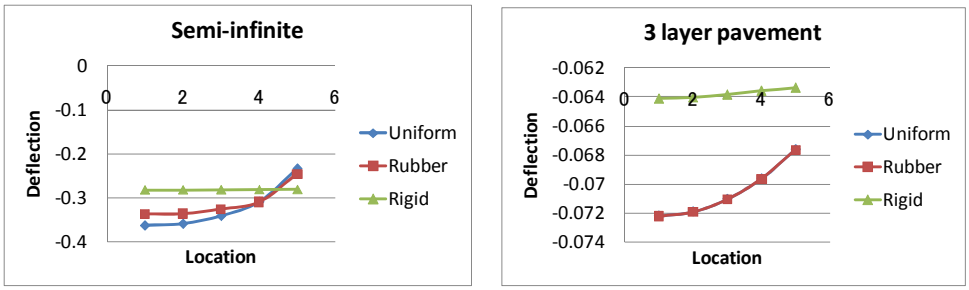

Figure 5: Deflection beneath the loading plate in each pavement model and loading plate type (Upper left: Uniformly distributed load, Upper right: Rubber type, Bottom: Rigid plate type).

5 DYNAMIC BACKCALCULATION USING IN-SITU FWD DATA

The dynamic response analysis using artificially generated FWD data was discussed above, and found that different pavement model and loading plate types affected on the response results. Now, dynamic backcalculation using actually measured FWD data in the field was carried out. The pavement model, here employed was 3 layer pavement model and loading plate types were uniformly distributed load, rubber, and rigid plate type as well as previous attempt. The filed pavement model was located at backyard in Tokyo Denki University, and its structural design component was based on heavy traffic road. This pavement consisted of, from the surface, dense graded asphalt concrete (modified polymer II type), course graded asphalt concrete, asphalt stabilized base, crusher run, and subgrade. To reduce the numerical expensiveness, the simplified 3 layer pavement model which combined all asphalt concrete layers to a unit layer, was developed (i.e., surface layer, base, and subgrade). The required input data for backcalculation were tabulated in Table 4. FWD load was 49 kN and radius of loading plate was 15 cm. FWD deflections were measured at 10:00 AM and the pavement temperature was 15.2 degrees Celsius. Dynamic backcalculation was executed for this pavement model, and each layer Young's modulus and damping coefficient were estimated. The densities were fixed as initial values and were not estimated.

For each loading type, the backcalculated Young's moduli for each layer are tabulated in Table 5. As shown in the table, the surface Young's modulus of uniformly distributed load is the largest and rigid plate type is the smallest. Additionally, Young's moduli of the uniformly distributed load and rubber type are similar, on the contrary, of the rigid plate is not close to those two values. Results of base and subgrade show the consistency for among all loading types.

Figure 6 shows time domain deflections at sensor locations on both actual FWD data and calculated data for each loading plate type. For all loading types, the actual FWD deflection data at each sensor and calculated deflection are matching well. Since the degree of matching is high, it can be said the dynamic backcalculation works correctly. Additionally, for all

loading types, the iterative numbers of dynamic backcalculation are less than 20, and CPU time for analysis is less than 1 minutes.

Table 4: Initial values of backcalculation for in-situ FWD data

	Layer 1	Layer 2	Layer 3
Layer thickness (cm)	25	35	60
Young's modulus (MPa)	7000	200	100
Damping Coef. (MPa-s)	35	1	0.5
Density (kg/m^3)	2300	1900	1600

Table 5: Backcalculated layer moduli for three layer asphalt concrete pavement using the in-situ FWD data regarding the loading plate types

	Uniformly distributed load type	Rubber type	Rigid plate type
Asphalt concrete layer	4755 MPa	4589 MPa	3531 MPa
Cement stabilized layer	96 MPa	106 MPa	109 MPa
Subgrade	300 MPa	287 MPa	302 MPa

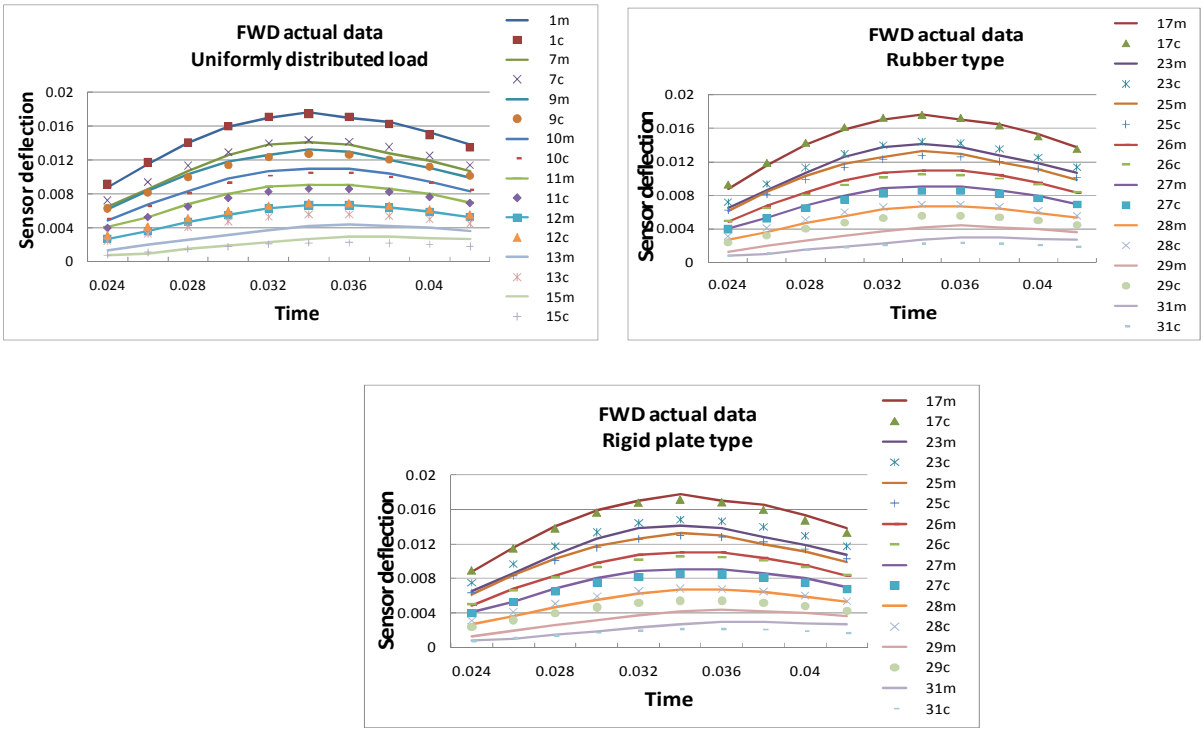

Figure 6: Time domain deflections at sensor locations on both actual FWD data and calculated data for each loading plate type (Upper left: Uniformly distributed load, Upper right: Rubber type, Bottom: Rigid plate type).

6 CONCLUSIONS

In this research, the effect of FWD loading plate to dynamic response and backcalculation analysis was investigated. Semi-infinite pavement model and 3 layer pavement models were developed with three different types of loading plate (uniformly distributed load, rubber, and rigid plate type) for numerical simulation. In the same way using 3 layer pavement models, dynamic backcalculation was carried out, and deflections under the loading plate were investigated for all cases above.

For semi-infinite model, the deflection of the loading plate edge became small in the uniformly distributed load and rubber type, and the deflections beneath the loading plate were not even distribution. On the other hand, the deflection became homogeneous distribution in the rigid plate type. In addition, time series deflection at the center of loading plate became small most in the rigid plate type, and became the maximum in the uniformly distributed load type. The amount of deflection of rubber type was between uniformly distributed load and rigid plate type.

A similar trend was observed for 3 layer pavement model, however the slight uneven distribution in rigid plated type was observed. This might be caused due to the fact that the pavement model is multi-layer system and its top layer is stiff. Similarly, the D0 deflection of rigid plate type was smaller than that of uniformly distributed load and rubber type.

The dynamic backcalculation analysis that used actual FWD data became an excellent analytical result in any types of loading plate. As for the estimated Young's modulus of surface layer, the rigid plate type showed the smallest Young's modulus and uniformly distributed load indicated the largest estimated value. Results of base and subgrade show the consistency for among all loading types.

Time series impact loading given by FWD device transmits the force to soil through the loading plate. However, there are still a lot of unsolved issues regarding the mechanism of transition. The shape and structural component of loading plate is different among standard FWD device and portable FWD device, hence further researches of effects of loading plate would be continued.

REFERENCES

1) Kikuta, Y., Matsui, K., Enya, T., and Abe, Y., 1997. Time Domain Backcalculation of Pavement Structure by Using Matrix Reduction, *Journal of Japan Society of Civil Engineers*, No.557/V-34, pp. 77-85.
2) Nishiyama, T., Matsui, K., Kikuta, Y., Higashi, S., 2008. Development of Estimated Method for Pavement Layer Densities, Damping Coefficient and Elastic Moduli, *Journal of Japan Society of Civil Engineers*, Vol.64, No.4, pp 572-579, 2008.